

Phospholipase D2 drives mortality in sepsis by inhibiting neutrophil extracellular trap formation and down-regulating CXCR2

Sung Kyun Lee,¹ Sang Doo Kim,¹ Minsoo Kook,¹ Ha Young Lee,^{1,2} Jaewang Ghim,³ Youngwoo Choi,³ Brian A. Zabel,⁴ Sung Ho Ryu,³ and Yoe-Sik Bae^{1,2,5}

¹Department of Biological Sciences, Sungkyunkwan University, Suwon 16419, Republic of Korea

²Mitochondria Hub Regulation Center, Dong-A University, Busan 49201, Republic of Korea

³Department of Life Sciences, Pohang University of Science and Technology, Pohang 37673, Republic of Korea

⁴Palo Alto Veterans Institute for Research, Veterans Affairs Hospital, Palo Alto, CA 94304

⁵Department of Health Sciences and Technology, Samsung Advanced Institute for Health Sciences and Technology, Sungkyunkwan University, Seoul 06351, Republic of Korea

We determined the function of phospholipase D2 (PLD2) in host defense in highly lethal mouse models of sepsis using PLD2^{-/-} mice and a PLD2-specific inhibitor. PLD2 deficiency not only increases survival but also decreases vital organ damage during experimental sepsis. Production of several inflammatory cytokines (TNF, IL-1 β , IL-17, and IL-23) and the chemokine CXCL1, as well as cellular apoptosis in immune tissues, kidney, and liver, are markedly decreased in PLD2^{-/-} mice. Bactericidal activity is significantly increased in PLD2^{-/-} mice, which is mediated by increased neutrophil extracellular trap formation and citrullination of histone 3 through peptidylarginine deiminase activation. Recruitment of neutrophils to the lung is markedly increased in PLD2^{-/-} mice. Furthermore, LPS-induced induction of G protein-coupled receptor kinase 2 (GRK2) and down-regulation of CXCR2 are markedly attenuated in PLD2^{-/-} mice. A CXCR2-selective antagonist abolishes the protection conferred by PLD2 deficiency during experimental sepsis, suggesting that enhanced CXCR2 expression, likely driven by GRK2 down-regulation in neutrophils, promotes survival in PLD2^{-/-} mice. Furthermore, adoptively transferred PLD2^{-/-} neutrophils significantly protect WT recipients against sepsis-induced death compared with transferred WT neutrophils. We suggest that PLD2 in neutrophils is essential for the pathogenesis of experimental sepsis and that pharmaceutical agents that target PLD2 may prove beneficial for septic patients.

CORRESPONDENCE

Yoe-Sik Bae:

yoesik@skku.edu

Abbreviations used: AST, aspartate aminotransferase; BAEE, *N*- α -benzoyl-L-arginine ethyl ester hydrochloride; BALF bronchoalveolar lavage fluid; [Ca²⁺]_i, intracellular calcium concentration; CLP, cecal ligation puncture; GRK2, G protein-coupled receptor kinase 2; MMK-1, Leu-Glu-Ser-Ile-Phe-Arg-Ser-Leu-Leu-Phe-Arg-Val-Met; NET, neutrophil extracellular trap; PAD, peptidylarginine deiminase; PLD2, phospholipase D2; TUNEL, terminal deoxynucleotidyl transferase dUTP nick end labeling; WKYMVm, Trp-Lys-Tyr-Met-Val-D-Met.

Sepsis is a systemic inflammatory response syndrome that results from infection of invading microorganisms and is associated with substantial clinical mortality in the United States (27%), with no effective therapy to improve patient survival (Angus et al., 2001; Cohen, 2002; Kumar et al., 2011).

Sepsis-induced mortality is closely linked with the failure of the host's innate immune response to contain and destroy invading pathogens (Hotchkiss et al., 2013). Neutrophils generate neutrophil extracellular traps (NETs) that can enmesh circulating bacteria from the bloodstream and provide intravascular immunity against septic infection (McDonald et al., 2012). Neutrophil recruitment to sites of infection is also important in controlling invading pathogens

(Alves-Filho et al., 2010). CXCR2 regulates neutrophil influx during infection and is down-regulated on neutrophils from septic patients (Cummings et al., 1999).

Phospholipase D2 (PLD2) is a crucial cell signaling enzyme in neutrophils and other cell types that hydrolyze phosphatidylcholine to phosphatidic acid and choline (Jang et al., 2012). Phosphatidic acid can bind and activate many different kinases, phosphatases, nucleotide-binding proteins, and phospholipases that control cell migration, proliferation, and activation

© 2015 Lee et al. This article is distributed under the terms of an Attribution-Noncommercial-Share Alike-No Mirror Sites license for the first six months after the publication date (see <http://www.rupress.org/terms>). After six months it is available under a Creative Commons License (Attribution-Noncommercial-Share Alike 3.0 Unported license, as described at <http://creativecommons.org/licenses/by-nc-sa/3.0/>).

(Jang et al., 2012). A functional role for PLD2 in the pathogenesis of sepsis has yet to be explored. We therefore investigated the role of PLD2 in multiple models of experimental sepsis.

RESULTS AND DISCUSSION

PLD2 deficiency increased survival rate and reduced vital organ inflammation against polymicrobial sepsis

To examine the role of PLD2 on the pathogenesis of polymicrobial sepsis, we first assessed survival after cecal ligation puncture (CLP)-induced polymicrobial sepsis in WT versus PLD2^{-/-} mice. PLD2 deficiency significantly improved the survival rate, with 90% of mice surviving by day 10 compared with just 25% of WT, suggesting that PLD2 plays a pathogenic role in endotoxemia (Fig. 1 a). The intestinal microbiomes were not fundamentally different between WT and PLD2^{-/-} mice (Fig. S1), indicating that the difference in susceptibility to CLP-induced mortality was not mediated by possible different intestinal microbiomes.

Staphylococcus aureus (*S. aureus*) is a Gram-positive bacterium that is a major contributor to sepsis in the clinic (Lowy, 1998). We therefore tested the effects of PLD2 deficiency on survival in a *S. aureus*-dependent sepsis model. Again, PLD2^{-/-} mice were significantly protected against *S. aureus*-mediated septic mortality, with 50% of mice surviving for 10 d compared with just 12.5% of WT mice (Fig. 1 b). Because PLD2 is constitutively

active (Colley et al., 1997), we next asked if a PLD2-specific inhibitor would also protect against sepsis-associated mortality. Survival was significantly extended in WT mice treated with the PLD2-selective inhibitor (*N*-[2-(4-oxo-1-phenyl-1,3,8-triazaspiro[4,5]dec-8-yl)ethyl]-2-naphthalenecarboxamide; Scott et al., 2009) compared with vehicle control (40 vs. 5% survival, respectively; Fig. 1 c). Collectively, these results strongly suggest that PLD2 (more precisely, PLD2 activity) is involved in the pathological progression of sepsis.

CLP-induced mouse mortality is closely associated with lung inflammation and dysfunction of vital organs, including the liver (Cohen, 2002). Histological analysis confirmed that CLP caused dramatic inflammation of the lungs, with severe alveolar congestion and extensive formation of thrombotic lesions in WT mice but not in PLD2^{-/-} mice (Fig. 1 d). CLP surgery significantly increased the lung wet/dry ratio in WT mice, indicating the presence of edema, which was not observed in PLD2^{-/-} mice (Fig. 1 e). Histological analysis also confirmed that CLP caused marked, time-dependent liver inflammation with severe damage 24 h after CLP in WT mice but not in PLD2^{-/-} mice (Fig. 1 f). Plasma aspartate aminotransferase (AST) levels (a marker of liver damage) were also significantly elevated in WT CLP mice at 12 and 24 h after induction compared with PLD2^{-/-} mice (Fig. 1 g).

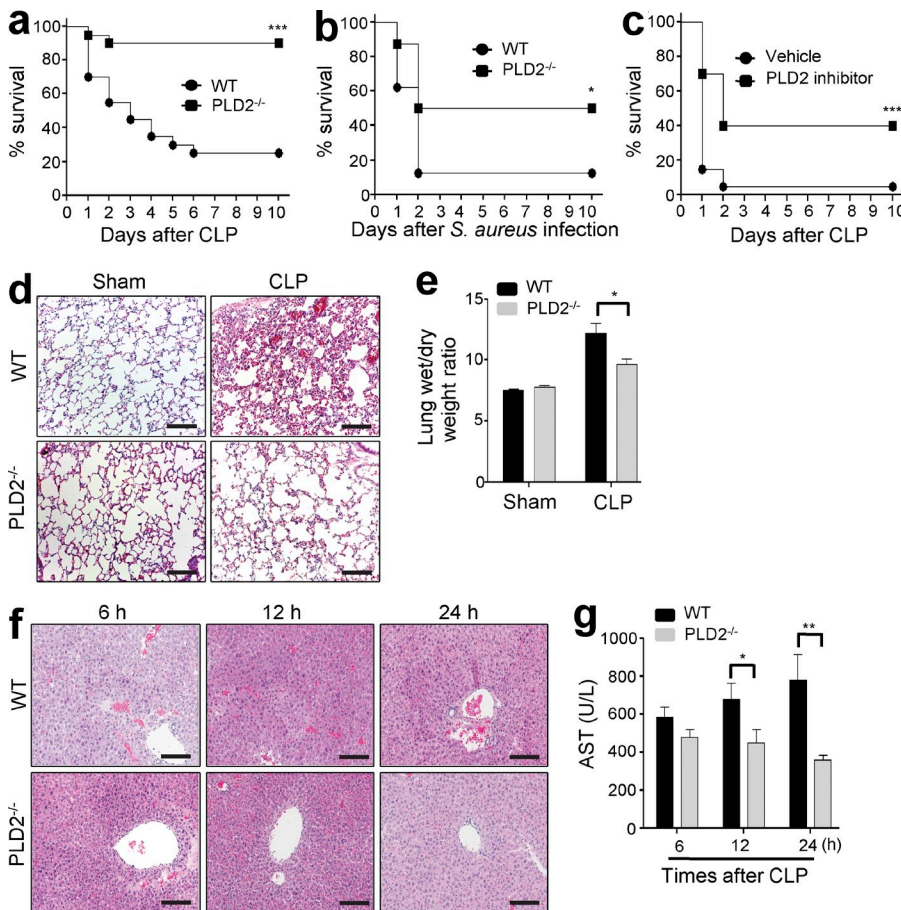


Figure 1. PLD2 is required for lethality and vital organ damage in CLP-induced sepsis. (a and c) WT or PLD2^{-/-} mice were subjected to CLP (a), or injected with *S. aureus* (2 × 10⁸; b), PLD2 inhibitor, or vehicle control (0.5% Tween 80 in PBS) was injected s.c. 4 times into mice 2, 14, 26, and 38 h after CLP (c). Survival was monitored for 10 d. *, P < 0.05; ***, P < 0.001, by ANOVA. Sample size, n = 20 per group (a and c); n = 8 per group (b). (d–g) WT or PLD2^{-/-} mice were subjected to CLP and were sacrificed 24 h after surgery. The lungs and livers were stained with hematoxylin and eosin (d and f). The data are representative of eight mice per group from two independent experiments. Bar, 100 μm (d and f). The lungs were used to measure the wet/dry weight ratio 24 h after CLP (e). The levels of plasma AST were measured (g). Mean ± SEM (n = 6; e and g). *, P < 0.05; **, P < 0.01 by t test. Data were pooled from two independent experiments (a–c). Data are representative of three independent experiments (e and g).

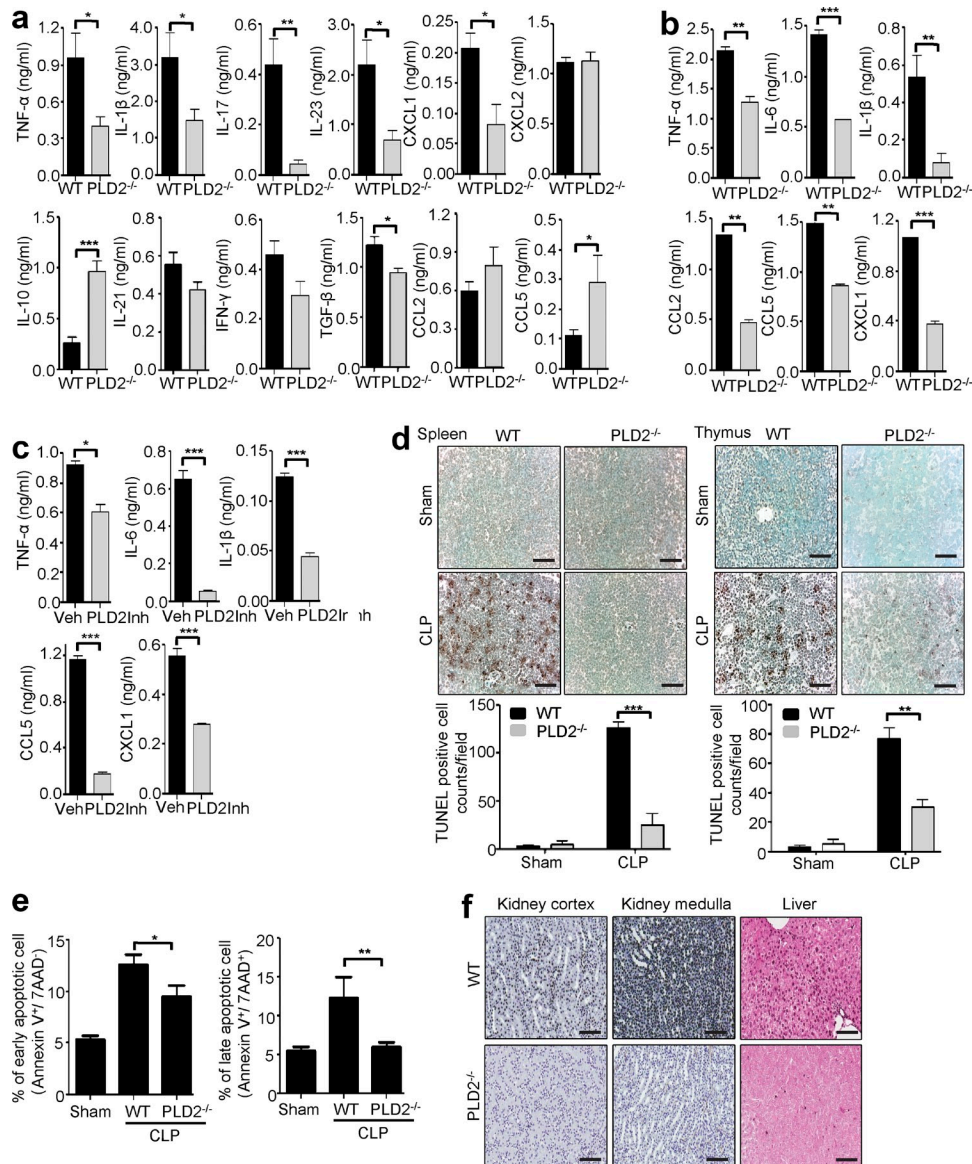


Figure 2. PLD2 is required for elevated inflammatory cytokines and lymphocyte apoptosis after CLP. (a) Cytokine levels in peritoneal fluid exudates from WT or PLD2^{-/-} mice were determined at 24 h after CLP. (b) Splenocytes isolated from WT or PLD2^{-/-} mice were stimulated with LPS (1 μg/ml) for 24 h. (c) Mouse splenocytes were stimulated with LPS (1 μg/ml) and PLD2 inhibitor (10 μM) or vehicle control (veh, 0.5% Tween 80 in PBS) for 24 h. The levels of cytokines were measured by ELISA (a–c). Mean ± SEM (n = 7 mice per group [a]; n = 3 mice [b and c]). *, P < 0.05; **, P < 0.01; ***, P < 0.001 by Student's *t* test. (d–f) WT or PLD2^{-/-} mice were subjected to CLP, and were sacrificed 24 h after surgery. The spleen, thymus, kidney, and liver were subjected to DNA fragmentation analysis (TUNEL). The data are representative of eight mice per group from two independent experiments (d [top] and f). Bar, 100 μm (d and f). TUNEL-positive cells were counted (d, bottom). Splenocyte death from CLP WT or PLD2^{-/-} mice was determined by flow cytometry using anti-Annexin V antibody and 7-AAD (e). Mean ± SEM (n = 8 [d]; n = 4 [e]). *, P < 0.05; **, P < 0.01; ***, P < 0.001 by Student's *t* test. Data are representative of two (a and e) or three (b–c and d [bottom]) independent experiments.

PLD2 deficiency decreased CLP-induced inflammatory cytokines/chemokines and apoptosis

We next asked if PLD2 deficiency was associated with a reduction in key cytokines involved in the pathogenic systemic inflammatory response syndrome triggered during sepsis. CLP surgery dramatically induced proinflammatory cytokine levels during the initial 24 h in peritoneal exudates from WT mice.

However, the levels of several proinflammatory cytokines (TNF, IL-1β, IL-17, and IL-23) and chemokine CXCL1 were significantly reduced in samples from CLP PLD2^{-/-} mice (Fig. 2 a). There were no genotype-dependent differences in several other cytokines (IL-21 and IFN-γ) or chemokines (CCL2 and CXCL2). Furthermore, IL-10 and CCL5 were increased in exudates from PLD2^{-/-} mice compared with WT

(Fig. 2 a). PLD2-deficient splenocytes or WT splenocytes treated with PLD2 inhibitor and then challenged with LPS *ex vivo* showed a similar trend in significantly reduced inflammatory cytokine and chemokine secretion compared with controls (Fig. 2, b and c). Collectively, the cytokine analysis indicates that PLD2 deficiency has a specific and selective effect on the production of key cytokines and chemokines that drive the pathology of polymicrobial sepsis.

Immune cell apoptosis is associated with sepsis-induced mortality (Cohen, 2002). CLP caused a marked increase in lymphocyte apoptosis in the spleen and in the thymus in WT, but not in PLD2^{-/-} mice, as measured by terminal deoxynucleotidyl transferase dUTP nick end labeling (TUNEL) histology (Fig. 2 d). Thus, PLD2 deficiency strongly attenuates lymphocyte apoptosis in the spleen and thymus, thereby contributing additional protective effects against sepsis-induced mortality. CLP also caused an increase in the Annexin V⁺/7-AAD⁻ or Annexin V⁺/7-AAD⁺ cell populations in WT mice, which was markedly decreased in PLD2^{-/-} mice (Fig. 2 e). CLP also caused a marked increase in renal cell apoptosis in the kidney cortex and medulla, and in liver hepatocytes in WT but not PLD2^{-/-} mice as determined by TUNEL histology (Fig. 2 f). These data indicate that vital organ injury is more severe in WT mice compared with PLD2^{-/-} mice.

PLD2 deficiency enhanced bactericidal activity by up-regulating NET formation through peptidylarginine deiminase (PAD) activation and augmenting phagocytic killing of bacteria

Septic mortality correlates with bacterial colony counts in peritoneal fluid and peripheral blood (Xiao et al., 2006). Bacterial colony counts were significantly decreased in peritoneal lavage fluid by ~60% 24 h after CLP from PLD2^{-/-} mice compared with WT mice (Fig. 3 a). Because neutrophils play a key bactericidal role in the CLP model, we measured the recruitment of neutrophils into the peritoneal cavity and found that significantly more neutrophils were recruited 6 h after CLP in PLD2^{-/-} mice versus WT (Fig. 3 b). The enhanced recruitment was not simply a result of elevated numbers of circulating neutrophils in the PLD2^{-/-} mice via increased granulopoiesis (Fig. 3 c and Fig. S2).

Bacteria colony counts in peripheral blood and in bronchoalveolar lavage fluid (BALF) were also markedly decreased in PLD2^{-/-} mice versus WT (Fig. 3 a). Bacteria released into the peritoneal cavity eventually make their way through the circulation and enter lung tissue, resulting in lung inflammation (Matute-Bello et al., 2001). Bacteria colony counts in lung tissues were also significantly decreased in PLD2^{-/-} mice versus WT (Fig. 3 a). Live bacterial colony numbers were significantly increased in liver and spleen 24 h after CLP in WT mice compared with PLD2^{-/-} mice (Fig. 3 a).

It was recently reported that neutrophils generate NETs to trap and kill invading bacteria (Brinkmann et al., 2004). To investigate the effect of PLD2 deficiency on NET formation, we stained neutrophils with SYTOX Green nucleic acid stain, a nonpermeable dye that stains nucleic acid,

a primary component of NETs. Stimulation of neutrophils isolated from WT mice with ionomycin induced NET formation (Fig. 3 d). Interestingly, NET formation was markedly increased in ionomycin-stimulated neutrophils isolated from PLD2^{-/-} mice (Fig. 3 d). Moreover, NET formation without ionomycin stimulation was slightly increased by neutrophils isolated from PLD2^{-/-} mice versus WT (Fig. 3 d). Ionomycin-stimulated NET formation by WT neutrophils was also further increased by treatment with a PLD2 inhibitor (Fig. 3 e).

Citrullination of histone is associated with NET formation (Wang et al., 2009). Because PLD2 deficiency resulted in increased NET formation by SYTOX Green nucleic acid staining, we next assessed the NETs for citrullinated histone 3 content. The level of citrullinated histone 3 was dramatically increased in neutrophils isolated from PLD2^{-/-} mice compared with WT (Fig. 3 f). In addition, ionomycin stimulation strongly increased histone 3 citrullination in PLD2^{-/-} mice compared with either unstimulated PLD2^{-/-} or ionomycin-stimulated WT neutrophils (Fig. 3 f). Peritoneal exudate histone 3 citrullination was markedly increased in PLD2^{-/-} mice after CLP compared with WT mice (Fig. 3 g). Increased levels of citrullinated histone 3 and NET formation were also detected in lung neutrophils from CLP-operated PLD2^{-/-} mice versus WT by immunofluorescence staining (Fig. 3 h). PAD4 catalyzes histone 3 citrullination (Li et al., 2010). Because histone 3 citrullination was up-regulated in neutrophils isolated from PLD2^{-/-} mice, we measured PAD activity in neutrophils. PAD activity was significantly enhanced in PLD2^{-/-} neutrophils compared with WT (Fig. 3 i). Increased PAD activity was also present in lung tissue of sham PLD2^{-/-} mice versus WT, as well as 2 h after CLP PLD2^{-/-} mice versus WT (Fig. 3 j). The aggregate of these results indicate that deficiency of PLD2 enhances PAD activity resulting in histone 3 citrullination and NET formation in neutrophils. Addition of PLD2 inhibitor also stimulated PAD activity and histone 3 citrullination in neutrophils (unpublished data), which supports the notion that PLD2 activity normally suppresses PAD activity and subsequent histone 3 citrullination *in vivo*. Because PAD can catalyze the citrullination of other histones, such as histone 4 (Wang et al., 2009), there may be additional histone citrullination events that contribute to PLD2 deficiency-induced NET formation.

Intracellular calcium ions are required for PAD4 activation, resulting in histone 3 citrullination and NET formation (Rohrbach et al., 2012). Ionomycin-stimulated calcium flux was enhanced in neutrophils from PLD2^{-/-} mice compared with WT (Fig. 3 k). In addition, a PLD2 inhibitor strongly enhanced ionomycin-induced intracellular calcium mobilization in WT neutrophils (Fig. 3 k). These results suggest that PLD2 may normally suppress activation-dependent calcium signaling in neutrophils and dampen calcium-dependent PAD enzymatic activity, resulting in decreased histone 3 citrullination and NET formation.

We also tested whether PLD2 deficiency affects bacterial phagocytosis and phagocytic killing of bacteria. Ionomycin

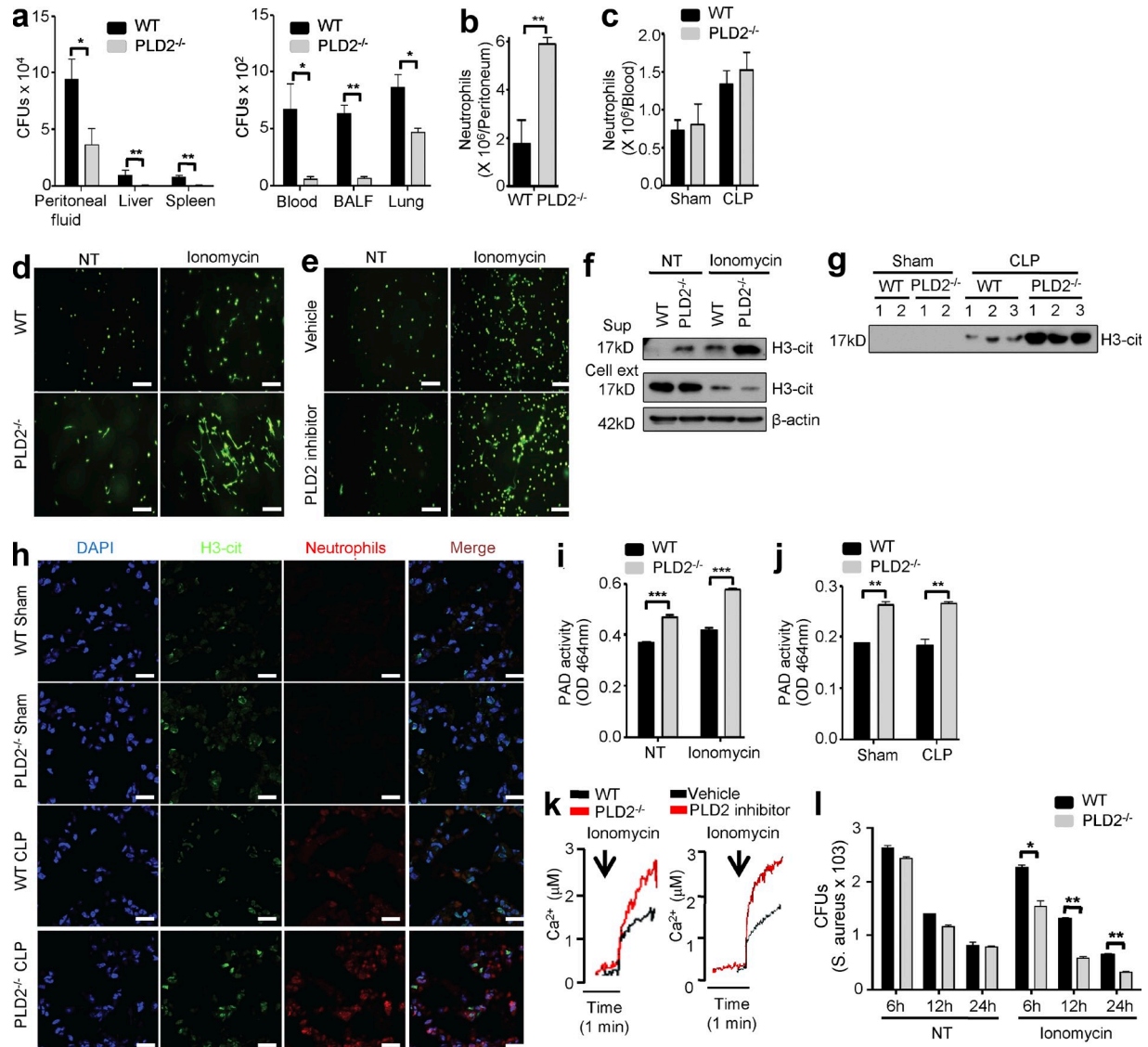


Figure 3. Increased bactericidal activity and NET formation in PLD2^{-/-} CLP mice. (a) WT or PLD2^{-/-} mice were subjected to CLP. Peritoneal lavage fluid, peripheral blood, BALF, lung, liver, and spleen were collected 24 h after CLP. The collected fluid samples or homogenized tissue samples were cultured overnight on blood-agar base plates at 37°C; the number of CFU was then determined. (b) WT or PLD2^{-/-} mice were subjected to CLP. 6 h after surgery, peritoneal fluids were collected and infiltrating neutrophils were enumerated by flow cytometry. (c) Circulating blood was collected from sham or CLP-operated WT or PLD2^{-/-} mice 6 h after surgery. Total blood neutrophils (Ly6G⁺) were counted by flow cytometry. (d and f) Neutrophils isolated from WT or PLD2^{-/-} mice were stimulated with ionomycin (5 μM) for 4 h. (e) Neutrophils from WT mice were stimulated with ionomycin (5 μM) for 4 h in the presence of PLD2 inhibitor (10 μM) or vehicle control (0.5% Tween 80 in PBS). NET formation was measured using SYTOX Green nucleic acid staining. Bar, 100 μm (d and e). Peritoneal fluid was harvested at 2 h from sham or CLP-operated WT or PLD2^{-/-} mice (g). Citrullinated histone 3 (H3-cit) levels were measured by Western blot analysis (f and g). WT or PLD2^{-/-} mice were subjected to CLP and sacrificed 2 h after surgery. The lungs were analyzed by immunofluorescence for the presence of neutrophils (red channel) or citrullinated histone 3 (green channel), with DAPI used to visualize DNA content. Bar, 100 μm (h). PAD activity was measured using BAEE as arginine derivative in mouse neutrophils (i) and harvested lung at 2 h after CLP (j). Neutrophils isolated from WT or PLD2^{-/-} mice were loaded with calcium-sensitive dye fura-2/AM and stimulated with ionomycin (2 μM) in the absence or presence of PLD2 inhibitor (10 μM; k). (l) Neutrophils isolated from WT or PLD2^{-/-} mice were incubated with *S. aureus* (2 × 10⁶) for 1 h, and phagocytic killing activity was measured. Mean ± SEM (n = 4 [a, i, and j]; n = 5 [b and c]; n = 3 [l]). *, P < 0.05; **, P < 0.01; ***, P < 0.001 by Student's *t* test. The data are representative of four different experiments (d–h and k). Data are representative of at least two independent experiments. NT, no treatment.

stimulated similar levels of phagocytosis (FITC-dextran uptake, 70 kD) in both of WT and PLD2^{-/-} neutrophils, suggesting that PLD2 deficiency likely does not affect bacterial phagocytosis (unpublished data). However, ionomycin-stimulated

phagocytic killing of bacteria was significantly increased by PLD2 deficiency (Fig. 3 l).

Collectively, our results suggest that PLD2 deficiency enhances bactericidal activity by stimulating both histone 3

citrullination–PAD activation–NET formation and phagocytic bacterial killing by neutrophils.

PLD2 deficiency elicits increased neutrophil recruitment to the lung by stabilizing CXCR2

Lung inflammation can be caused by live bacteria in sepsis (Xiao et al., 2006). Live bacteria released from CLP surgery may enter the blood stream, move into the lung, and subsequently enter the airways (Xiao et al., 2006). Because live bacterial colony numbers in BALF were markedly decreased after CLP in PLD2^{-/-} mice compared with WT (Fig. 3 a), and phagocytic cells mediate killing of bacteria, we compared the BALF leukocyte population in WT and PLD2^{-/-} mice. Interestingly, the total number of BALF leukocytes was significantly higher in PLD2^{-/-} mice versus WT (Fig. 4 a). Neutrophils were strongly recruited into the respiratory tract in PLD2^{-/-} mice compared with WT after CLP (Fig. 4 a).

The surface expression of CXCR2, which is a crucial factor in controlling recruitment of neutrophils into event areas, is decreased on neutrophils from septic patients compared with healthy individuals (Cummings et al., 1999; Alves-Filho et al., 2010). The expression level of CXCR2 was significantly higher on neutrophils from PLD2^{-/-} mice compared with WT in CLP-operated models (Fig. 4 b). The surface expression level of CXCR2 on WT neutrophils was significantly decreased 1 h after LPS treatment (Fig. 4 c and not depicted). Interestingly, however, LPS did not trigger down-regulation of CXCR2 on neutrophils from PLD2^{-/-} mice, especially compared with the effect of LPS on WT neutrophil CXCR2 levels (Fig. 4 c). Furthermore, LPS stimulation attenuated CXCR2-mediated WT neutrophil chemotaxis to CXCL2 and CXCL1, but the inhibitory effect of LPS on cell migration was significantly diminished in PLD2^{-/-} neutrophils (Fig. 4 d). Neutrophil chemotaxis to other chemoattractants (e.g., fMLP, Leu-Glu-Ser-Ile-Phe-Arg-Ser-Leu-Leu-Phe-Arg-Val-Met [MMK-1], Trp-Lys-Tyr-Met-Val-D-Met [WKYMVm], and C5a) was not affected by LPS or by PLD2 deficiency (Fig. 4 d). Surface-expressed CXCR2 is down-regulated in a phosphorylation-dependent manner, and G protein-coupled receptor kinase 2 (GRK2) has been reported to phosphorylate CXCR2 (Angus et al., 2001). We tested the effect of PLD2 deficiency on the expression of GRK2 induced by LPS. GRK2 expression was induced after 1 h of incubation with LPS in WT mice (Fig. 4 e and not depicted). However, LPS-stimulated GRK2 up-regulation was attenuated in neutrophils isolated from PLD2^{-/-} mice (Fig. 4 e). Collectively, PLD2 play an important role in the regulation of surface expression of CXCR2 by regulating the expression of GRK2 in mouse neutrophils. The regulatory mechanism of LPS-induced GRK2 expression in mouse neutrophils was tested using pharmacological inhibitors of intracellular signaling pathways. LPS-induced GRK2 expression was completely inhibited by IκBα inhibitor BAY11-7082, suggesting that it is an NF-κB-dependent process (Fig. 4 f). The activation of NF-κB is associated with p65 nuclear translocation (Maguire et al., 2011). Stimulation of WT neutrophils with LPS elicited p65 nuclear

translocation (Fig. 4 g). However, LPS-induced p65 nuclear translocation was markedly attenuated in neutrophils from PLD2^{-/-} mice (Fig. 4 g). This result suggests that PLD2 is required for the activation of NF-κB (an important transcription factor for the expression of GRK2) by LPS in mouse neutrophils. Moreover, LPS-induced CXCR2 down-regulation was significantly attenuated by BAY11-7082 (Fig. 4 h). BAY11-7082 treatment also partially but significantly rescued CXCL2-induced chemotactic migration of LPS-stimulated neutrophils (Fig. 4 i). We then tested the functional role of CXCR2 on the increased survival rate in PLD2^{-/-} mice challenged with CLP sepsis. The protective effect of PLD2 deficiency was abolished by treatment with CXCR2 antagonist SB225002 (Fig. 4 j). This result suggests that the increased survival rate in PLD2^{-/-} mice against sepsis is mediated by the effects of PLD2 deficiency in stabilizing and/or maintaining CXCR2 surface expression.

Neutrophils play a key role in PLD2-driven mortality in sepsis

Because global PLD2 deficiency strongly attenuated sepsis-induced lethality, we next asked if neutrophil-restricted PLD2 embodied the pathogenic effects of the enzyme. Mouse neutrophils isolated from WT or PLD2^{-/-} mice were adoptively transferred into neutrophil-depleted (anti-Ly6G-treated) WT recipients that were subsequently challenged with CLP-induced polymicrobial sepsis. Bacterial colony counts in peritoneal fluid were markedly decreased in recipient mice that received PLD2^{-/-} neutrophils compared with recipients that received WT neutrophils (Fig. 5 a). Lung inflammation and splenocyte apoptosis were significantly reduced in CLP mice that received PLD2^{-/-} versus WT neutrophils (Fig. 5, b and c). The levels of proinflammatory cytokines (TNF, IL-6, and IL-1β) and inflammatory chemokines (CCL2, CCL5, and CXCL1) in peritoneal fluid and BALF were also significantly reduced in CLP mice that received PLD2^{-/-} versus WT neutrophils (Fig. 5, d and e). Because the total number of airway-infiltrating neutrophils was significantly higher in CLP mice with a global deficiency in PLD2^{-/-} compared with WT (Fig. 4 a), we next asked if neutrophil-restricted PLD2 deficiency drives this phenotype. We labeled neutrophils from WT or PLD2^{-/-} mice with CFSE and adoptively transferred the cells into neutrophil-depleted WT CLP recipients by i.v. injection. In vivo neutrophil trafficking into the airways was then quantified by flow cytometry. PLD2^{-/-} neutrophils were more efficiently recruited into the airways than transferred WT neutrophils (Fig. 5 f). Finally, adoptively transferred PLD2^{-/-} neutrophils into neutrophil-depleted WT recipients significantly protected against CLP-induced death compared with transferred WT neutrophils (Fig. 5 g). In contrast, adoptive transfer of WT neutrophils into neutrophil-depleted PLD2^{-/-} recipients induced significant mortality in the CLP model (Fig. 5 h). Together the results strongly indicate that the protective effect of PLD2 deficiency against experimental sepsis is mediated by neutrophils.

We also compared the recruitment of CFSE-labeled WT and PLD2^{-/-} neutrophils in nondepleted WT mice. We

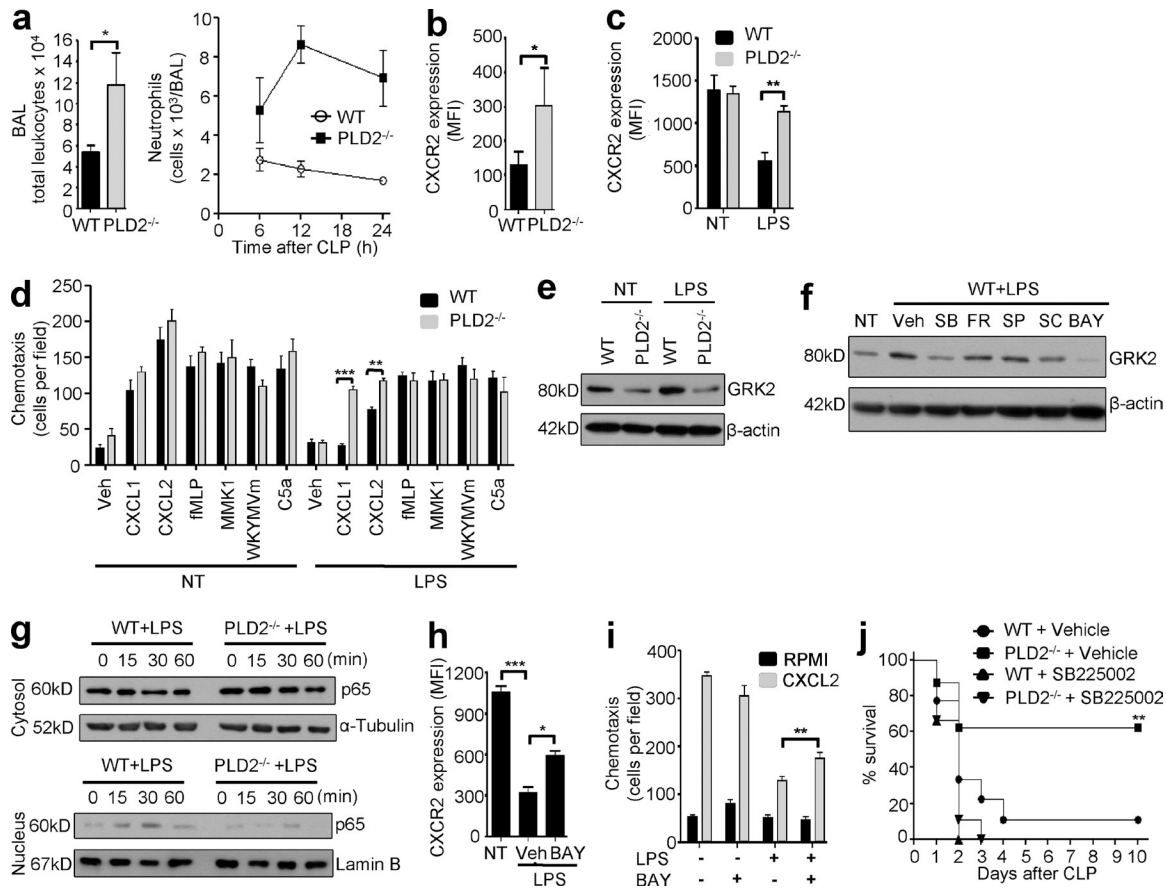


Figure 4. PLD2 inhibits neutrophil recruitment into the lung during CLP sepsis via CXCR2 down-regulation. (a and b) WT or PLD2^{-/-} mice were subjected to CLP. 6, 12, and 24 h after CLP (6 h after CLP for a [left] and b), BALF were collected and analyzed for the detection of total leukocytes and neutrophils by flow cytometry (a). (c–e) Neutrophils from WT or PLD2^{-/-} mice were left untreated or stimulated with LPS (1 μg/ml) for 1 h. Surface expression of CXCR2 in neutrophils was analyzed flow cytometry (b and c). Neutrophil chemotaxis toward vehicle (DMSO), CXCL1 (100 ng/ml), CXCL2 (30 ng/ml), fMLP (1 μM), MMK-1 (1 μM), WKYMVm (1 μM), or C5a (10 nM) was measured (d). (f) Neutrophils from WT mice were stimulated with LPS (1 μg/ml) for 1 h in the presence of vehicle (Veh, DMSO), SB203580 (SB, 30 μM), FR180204 (FR, 30 μM), SP600125 (SP, 30 μM), SC-514 (SC, 5 μM), or BAY11-7082 (BAY, 10 μM). The levels of GRK2 and β-actin were measured by Western blot analysis (e and f). (g) Neutrophils from WT or PLD2^{-/-} mice were stimulated with LPS (1 μg/ml) for 0, 15, 30, or 60 min. After fractionation, cytosolic and nuclear fractions were separated on SDS-PAGE, and the levels of p65 and α-Tubulin or Lamin B were determined by Western blot analysis (g). (h and i) Neutrophils were incubated with LPS (1 μg/ml) for 1 h in the presence of vehicle (DMSO) or BAY11-7082 (10 μM). Surface expression of CXCR2 was measured by flow cytometric analysis (h). CXCL2-induced chemotactic migration of neutrophils was evaluated (i). Mean ± SEM (n = 6 mice [a and b]; n = 3 [c, d, h, and i]). *, P < 0.05; **, P < 0.01; ***, P < 0.001 by Student's t test. (j) CXCR2 antagonist SB225002 (17.5 mg/kg) or vehicle (1% DMSO in PBS) was injected s.c. 2 h before CLP in WT or PLD2^{-/-} mice. Survival was monitored for 10 d. **, P < 0.01 comparing PLD2^{-/-} + vehicle versus PLD2^{-/-} + SB225002 by ANOVA. Sample size, n = ~7–9 mice per group. Data are representative of at least two independent experiments (a–i). Data were pooled from two independent experiments (j). NT, no treatment.

found that CFSE-labeled PLD2^{-/-} neutrophils were more effectively recruited into the airways than WT neutrophils (unpublished data), consistent with our result using neutrophil-depleted recipients. However, adoptive transfer of WT neutrophils into nondepleted PLD2^{-/-} mice did not worsen sepsis (unpublished data). Together with our previous results, the result suggests that PLD2^{-/-} neutrophils can overcome the pathogenic effects of transferred WT neutrophils in experimental sepsis.

In this study, we demonstrated that genetic or pharmaceutical targeting of PLD2 effectively prevented the progression of sepsis in the CLP polymicrobial sepsis model by enhancing

neutrophil recruitment and NET formation. Thus, our pre-clinical data support targeting PLD2 to limit the pathomechanisms that drive endotoxemia.

MATERIALS AND METHODS

Mice and CLP experimental sepsis model. C57BL/6 mice were purchased from Orient Bio. PLD2^{-/-} mice were generated as described previously (Ghim et al., 2014). All experiments involving animals received the approval of the Institutional Review Committee for Animal Care and Use at Sungkyunkwan University School of Medicine (Suwon, Korea). Experimental CLP sepsis model was conducted as described previously (Kim et al., 2011). In brief, mice were anesthetized with intraperitoneal injections of Zoletil (50 mg/kg) and Rompun (10 mg/kg), after which a small abdominal

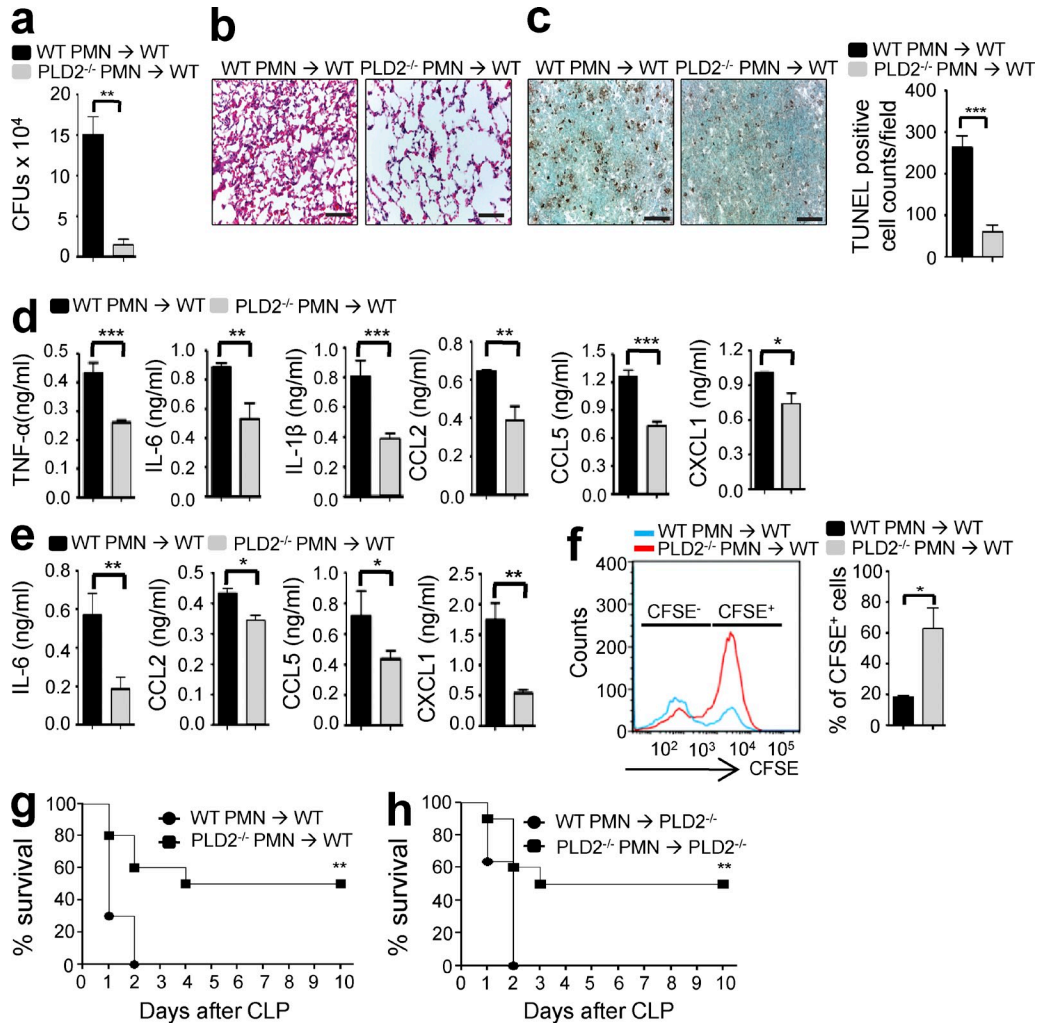


Figure 5. Adoptive transfer of neutrophils isolated from PLD2^{-/-} mice protects against CLP. (a–e and g) Neutrophils isolated from WT or PLD2^{-/-} mice were adoptively transferred to neutrophil-depleted WT recipient mice before CLP. Peritoneal lavage fluid was collected 24 h after CLP, and the number of CFU was then determined (a). The mice were sacrificed 24 h after surgery (b–e). The lungs were stained with hematoxylin and eosin (b). The spleens were subjected to DNA fragmentation analysis (TUNEL). The data are representative of eight mice per group from two independent experiments (b and c, left). Bar, 100 μm (b and c). TUNEL-positive cells were counted (c right). (d and e) Cytokine levels in peritoneal fluid exudates (d) or BALF (e) from mice receiving transferred WT or PLD2^{-/-} neutrophils were determined 24 h after CLP. (f) Neutrophils isolated from WT or PLD2^{-/-} CLP mice were labeled with CFSE, and adoptively transferred into neutrophil-depleted WT mice. After CLP surgery in the recipient mice, recruited airway neutrophils were analyzed by flow cytometric analysis. (h) Neutrophils isolated from WT or PLD2^{-/-} mice were adoptively transferred to neutrophil-depleted PLD2^{-/-} recipient mice before CLP. Mean ± SEM (n = 6 for a, c [right], d, and e; n = 3 for f [right]). *, P < 0.05; **, P < 0.01; ***, P < 0.001 by Student's t test. Survival was monitored in adoptive transfer recipient CLP mice for 10 d. **, P < 0.01 by ANOVA. Sample size, n = 10–11 mice per group (g and h). Data are representative of two independent experiments (a and c, right; d, e, and f, right) or were pooled from two independent experiments (g and h).

midline incision was made to expose the cecum. The cecum was then ligated below the ileocecal valve and punctured twice through both surfaces (or once for the measurement of cytokine production) with a 22-gauge needle, and then the abdomen was closed. Sham CLP mice were subjected to the same procedure, but without puncture of the cecum. For the *S. aureus* model, *S. aureus* (2 × 10⁸ cells per mouse) was injected i.p. Vehicle (0.5% Tween 80 in PBS) or PLD2 inhibitor (4 mg/kg) was injected s.c. 4 times into CLP mice 2, 14, 26, and 38 h after CLP. Survival was monitored daily for 10 d.

Tissue histology. WT or PLD2^{-/-} mice were subjected to sham or CLP surgery. The mice were killed 12 or 24 h after surgery, after which their lungs and livers were fixed, sectioned, and stained with hematoxylin and eosin for morphological analysis.

Quantification of pulmonary edema. The extent of pulmonary edema was quantified by measuring the wet/dry weight ratio of the lung as previously described (Kim et al., 2011). The mice were killed 24 h after sham or CLP surgery. Whole harvested wet lungs were then weighed and placed in an oven for 48 h at 60°C. The dry weight was then measured and the wet/dry weight ratio was calculated.

Measurement of AST levels. The levels of AST were measured using commercially available kits (Sigma-Aldrich) according to standard laboratory techniques (Horder et al., 1981).

Measurement of cytokines in CLP model. To measure the production of CLP-induced cytokines in peritoneal lavage fluids, WT or PLD2^{-/-} mice

were subjected to sham or CLP surgery. The peritoneal lavage fluids were collected 24 h after surgery, and the cytokines present in the peritoneal fluid were measured by ELISA (eBioscience).

Measurement of cytokines from inflammatory cells in vitro. Mouse splenocytes (3×10^6 cells/0.3 ml) isolated from WT or PLD2^{-/-} mice were placed in RPMI 1640 medium containing 5% fetal bovine serum in 96-well plates and kept in a 5% CO₂ incubator at 37°C. The freshly isolated splenocytes were then incubated with LPS (1 µg/ml) for 24 h. To test the effect of PLD2 inhibitor on the production of cytokines, splenocytes were incubated with PLD2 inhibitor (10 µM) for 30 min before addition of LPS (1 µg/ml) for 24 h. The cell-free supernatants were then collected, centrifuged, and measured for each cytokine by ELISA (eBioscience) according to the manufacturer's instructions.

TUNEL assay. WT or PLD2^{-/-} mice were subjected to sham or CLP surgery. The mice were euthanized 24 h after surgery, after which their spleens, thymi, kidneys, and livers were isolated. The TUNEL assay was performed on frozen tissue sections using a standard histological protocol. In brief, the sections were permeabilized with Triton X-100 at 4°C for 2 min and flooded with TUNEL reagent for 60 min at 37°C. The percentage of apoptotic (TUNEL-positive) cells was evaluated by counting 500 total cells under a light microscope.

Assessment of splenic cell apoptosis by flow cytometric analysis. WT or PLD2^{-/-} mice were subjected to sham or CLP surgery. The mice were euthanized 24 h after surgery, after which their spleens were isolated. Splenic cell apoptosis was determined by Annexin-V/7-AAD-positive staining. Annexin-V/7-AAD co-staining was performed using the Annexin-V-FITC/7-AAD kit from Beckman Coulter and analyzed on a FACSCanto II flow cytometer (BD).

Measurement of CFUs in CLP model. WT or PLD2^{-/-} mice were subjected to CLP surgery. 24 h after CLP, peritoneal lavage fluid, peripheral blood, and BALF were collected and cultured overnight on blood-agar base plates (Trypticase Soy Agar Deeps; BD) at 37°C. The lungs, livers, and spleens were also isolated, and 10 mg of each tissue was homogenized in 700 µl of PBS. 50 µl of the tissue homogenate was then cultured overnight on blood-agar plates at 37°C. CFUs were determined as described previously (Kim et al., 2011).

Isolation of mouse bone marrow neutrophils. Bone marrow cells were isolated from femurs and tibias with HBSS-EDTA solution. The cell suspension was centrifuged at 400 g for 10 min. Next, resuspended cells were carefully loaded on a 52%, 69%, 78% Percoll gradient, and centrifuged at 1,500 g for 30 min without braking. Cells were isolated on the 69%/78% interface layer, and RBCs were removed by hypotonic lysis. Isolated cells were over 95% Ly6G-positive by flow cytometry (FACSCanto II; BD).

Fluorescence microscopy of NET formation. Mouse bone marrow neutrophils were isolated from WT or PLD2^{-/-} mice. Neutrophils (10^5 cells) were seeded on 12-mm 0.01% poly-L-lysine-coated coverslips in 24-well plates and were stimulated with ionomycin (5 µM). Cells were fixed with 4% paraformaldehyde and then stained with SYTOX Green nucleic acid stain (5 µM). NETs were visualized on an Axiovert fluorescence microscope (Carl Zeiss) and images were taken using a Nikon digital camera.

Detection of histone 3 citrullination levels from peritoneal fluid. WT or PLD2^{-/-} mice were subjected to sham or CLP surgery. 2 h after CLP, peritoneal fluid was collected, and secreted proteins in supernatants were precipitated by adding 1 volume of chloroform and 4 volumes of methanol. The proteins at the liquid interface were collected and dried using speed-Vac. Then proteins were separated by SDS-PAGE and transferred to a polyvinylidene difluoride membrane (Millipore). The levels of citrullinated histone 3 were detected using anti-histone H3 (citrulline R2 + R8 + R17) antibodies (Abcam).

Immunofluorescence histochemistry. WT or PLD2^{-/-} mice were subjected to CLP surgery. The mice were euthanized 2 h after surgery. Isolated lung was embedded in optimal cutting temperature compound. Lung sections were fixed with methanol for 10 min at -20°C. After blocking each section with blocking solution (PBS with 10% normal goat serum, 0.01% Triton X-100) for 1 h at room temperature, neutrophils and citrullinated histone 3 were detected with rat anti-NIMP-R14 and rabbit anticitrullinated histone H3 (Abcam), respectively. Anti-rat IgG AF594 and anti-rabbit IgG AF488 (Invitrogen) were used as secondary antibodies. DNA was stained with DAPI (Santa Cruz Biotechnology, Inc.) and mounted on a glass slide. Cells were visualized using an LSM 500 (Carl Zeiss).

Measurement of PAD activity. PAD activity was determined by colorimetric measurement of citrulline generated by PAD-catalyzed citrullination of BAEE (*N*- α -Benzoyl-L-arginine ethyl ester hydrochloride). 10 µg of cell lysate or lung extract was reacted by adding 5 mM BAEE at 55°C, and stopped 30 min later with the addition of 25 µl 5M HClO₄. Then supernatant was assayed for citrulline by mixing with reagent A (0.5% wt/vol diacetyl monoxime and 15% wt/vol NaCl in water) and reagent B (1% wt/vol antipyrine, 0.15% wt/vol ferric chloride, 25% vol/vol H₂SO₄ and 25% vol/vol H₃PO₄). The mixtures were boiled for 15 min and cooled on ice. The absorbance of the reagent mixtures at 464 nm was measured.

Calcium measurement. Intracellular calcium concentration ([Ca²⁺]_i) was measured according to Grynkiewicz's method using fura-2/AM as described previously (Grynkiewicz et al., 1985). In brief, freshly isolated mouse neutrophils were incubated with 3 µM fura-2/AM at 37°C for 50 min under continuous stirring. Next, the cells were aliquoted for each assay (2×10^6 cells/1 ml of Locke's solution containing 154 mM NaCl, 5.6 mM KCl, 1.2 mM MgCl₂, 5 mM Hepes, pH 7.3, 10 mM glucose, and 2 mM CaCl₂). The cells were stimulated with 2 µM ionomycin. Using excitation wavelengths of 340 and 380 nm, fluorescence changes were measured at an emission wavelength of 500 nm using a RF-5301PC spectrofluorophotometer (Shimadzu Instruments Inc.). An increase in [Ca²⁺]_i caused an increase in the fluorescence ratio of 340 to 380 nm excitation efficiency, and [Ca²⁺]_i was calculated using the fluorescence ratio according to eq. 5 of Grynkiewicz et al. (Grynkiewicz et al., 1985).

Measurement of phagocytic bacteria-killing activity. Neutrophils isolated from WT or PLD2^{-/-} mice were incubated with *S. aureus* (2×10^6) for 1 h, and then nonengulfed bacteria were killed with 100 µg/ml gentamicin for 1 h. Neutrophils were stimulated with ionomycin (5 µM) for 6, 12, or 24 h. Intracellular bacteria were measured by lysis of neutrophils and plating on Trypticase Soy Agar.

Assessment of leukocytes from peritoneal fluid or BALF in CLP mice. WT or PLD2^{-/-} mice were subjected to CLP surgery. The mice were then euthanized 6, 12, or 24 h after surgery. Peritoneal fluids were collected. To obtain BALF, tracheas were cannulated after exsanguination and the airways were lavaged with 900 µl of PBS. BALF samples were centrifuged (300 g, 10 min) to isolate cells. Total cells from lung were stained with anti-CD11b (M1/70) antibody. Neutrophils were stained with anti-Ly-6G (1A8). The cells were read by FACSCanto II flow cytometer and data were analyzed by FlowJo 7.6.5.

Assessment of CXCR2 level from neutrophils in vivo and in vitro. WT or PLD2^{-/-} mice were subjected to CLP surgery. The mice were then euthanized 6 h after surgery. Cells were collected from BALF and stained with the following antibodies: CD11b (M1/70), Ly-6G (1A8) from eBioscience and CXCR2 (TG11/CXCR2) from BioLegend. Bone marrow neutrophils were isolated from WT or PLD2^{-/-} mice. Cells were stimulated with 1 µg/ml of LPS for 1 h, and then stained and analyzed by flow cytometry (FACSCanto II; BD).

Measurement of p65 translocation by Western blot. For subcellular fractionation, the subcellular Protein Fraction kit (Thermo Fisher Scientific)

was used. Cellular compartments were continually extracted with cytoplasmic extraction buffer followed by nuclear extraction buffer. Proteins were separated by SDS-PAGE and transferred onto nitrocellulose membranes. The levels of p65, α -tubulin, and lamin B were detected using antibodies against each protein.

Neutrophil depletion and adoptive transfer experiment. For the adoptive transfer of neutrophils, recipient WT mice were injected i.p. with 500 μ g α Ly6G antibody (1A8; BioXCell) 24 and 2 h before CLP surgery. Neutrophil depletion was assessed by flow cytometry after staining peripheral blood neutrophils with anti-CD11b and anti-Ly-6G, and >99% recipient neutrophils were depleted. Isolated neutrophils (2×10^6) from WT or PLD2^{-/-} bone marrow were injected i.v. (tail vein) into neutrophil-depleted WT or PLD2^{-/-} recipient mice after CLP surgery. For the in vivo trafficking experiments, neutrophils from WT or PLD2^{-/-} mice were labeled with CFSE (green; 5 μ M; Invitrogen), incubating at 37°C for 15 min. The labeled neutrophils were injected by tail vein into neutrophil-depleted WT recipient mice after CLP induction. CFSE-labeled neutrophils from WT or PLD2^{-/-} donors were quantified in recipient BALF 6 h after CLP by flow cytometry (FACSCanto II; BD).

Online supplemental material. Fig. S1 summarizes pyrosequencing analysis of intestinal microbiota from WT and PLD2^{-/-} mice. Fig. S2 summarizes comparison of granulopoiesis from WT and PLD2^{-/-} mice. Online supplemental material is available at <http://www.jem.org/cgi/content/full/jem.20141813/DC1>.

This study was supported by grants from the Korean Health Technology R&D Project, Ministry of Health and Welfare, Republic of Korea (HI13C1857; Y.-S. Bae), and the National Research Foundation of Korea (2015 008728 [Y.-S. Bae], 2013H1A8A1004025 [S.K. Lee]). B.A. Zabel was supported by National Institutes of Health grant AI-079320. S.K. Lee, S.D. Kim, and Y.-S. Bae are pending patent application.

The authors declare no competing financial interests.

Submitted: 18 September 2014

Accepted: 17 July 2015

REFERENCES

- Alves-Filho, J.C., F. Sônego, F.O. Souto, A. Freitas, W.A. Verri Jr., M. Auxiliadora-Martins, A. Basile-Filho, A.N. McKenzie, D. Xu, F.Q. Cunha, and F.Y. Liew. 2010. Interleukin-33 attenuates sepsis by enhancing neutrophil influx to the site of infection. *Nat. Med.* 16:708–712. <http://dx.doi.org/10.1038/nm.2156>
- Angus, D.C., W.T. Linde-Zwirble, J. Lidicker, G. Clermont, J. Carcillo, and M.R. Pinsky. 2001. Epidemiology of severe sepsis in the United States: analysis of incidence, outcome, and associated costs of care. *Crit. Care Med.* 29:1303–1310. <http://dx.doi.org/10.1097/00003246-200107000-00002>
- Brinkmann, V., U. Reichard, C. Goosmann, B. Fauler, Y. Uhlemann, D.S. Weiss, Y. Weinrauch, and A. Zychlinsky. 2004. Neutrophil extracellular traps kill bacteria. *Science*. 303:1532–1535. <http://dx.doi.org/10.1126/science.1092385>
- Cohen, J. 2002. The immunopathogenesis of sepsis. *Nature*. 420:885–891. <http://dx.doi.org/10.1038/nature01326>
- Colley, W.C., T.C. Sung, R. Roll, J. Jenco, S.M. Hammond, Y. Altshuler, D. Bar-Sagi, A.J. Morris, and M.A. Frohman. 1997. Phospholipase D2, a distinct phospholipase D isoform with novel regulatory properties that provokes cytoskeletal reorganization. *Curr. Biol.* 7:191–201. [http://dx.doi.org/10.1016/S0960-9822\(97\)70090-3](http://dx.doi.org/10.1016/S0960-9822(97)70090-3)
- Cummings, C.J., T.R. Martin, C.W. Frevert, J.M. Quan, V.A. Wong, S.M. Mongovin, T.R. Hagen, K.P. Steinberg, and R.B. Goodman. 1999. Expression and function of the chemokine receptors CXCR1 and CXCR2 in sepsis. *J. Immunol.* 162:2341–2346.
- Ghim, J., J.S. Moon, C.S. Lee, J. Lee, P. Song, A. Lee, J.H. Jang, D. Kim, J.H. Yoon, Y.J. Koh, et al. 2014. Endothelial deletion of phospholipase D2 reduces hypoxic response and pathological angiogenesis. *Arterioscler. Thromb. Vasc. Biol.* 34:1697–1703. <http://dx.doi.org/10.1161/ATVBAHA.114.303416>
- Gryniewicz, G., M. Poenie, and R.Y. Tsien. 1985. A new generation of Ca²⁺ indicators with greatly improved fluorescence properties. *J. Biol. Chem.* 260:3440–3450.
- Horder, M., W. Gerhardt, M. Härkönen, E. Magid, E. Pitkänen, J.H. Strömme, L. Theodorsen, and J. Waldenström. 1981. Experiences with the Scandinavian recommended methods for determinations of enzymes in blood. A report by the Scandinavian Committee on Enzymes (SCE). *Scand. J. Clin. Lab. Invest.* 41:107–116. <http://dx.doi.org/10.3109/00365518109092022>
- Hotchkiss, R.S., G. Monneret, and D. Payen. 2013. Sepsis-induced immunosuppression: from cellular dysfunctions to immunotherapy. *Nat. Rev. Immunol.* 13:862–874. <http://dx.doi.org/10.1038/nri3552>
- Jang, J.H., C.S. Lee, D. Hwang, and S.H. Ryu. 2012. Understanding of the roles of phospholipase D and phosphatidic acid through their binding partners. *Prog. Lipid Res.* 51:71–81. <http://dx.doi.org/10.1016/j.plipres.2011.12.003>
- Kim, S.D., H.Y. Lee, J.W. Shim, H.J. Kim, Y.H. Yoo, J.S. Park, S.H. Baek, B.A. Zabel, and Y.S. Bae. 2011. Activation of CXCR2 by extracellular matrix degradation product acetylated Pro-Gly-Pro has therapeutic effects against sepsis. *Am. J. Respir. Crit. Care Med.* 184:243–251. <http://dx.doi.org/10.1164/rccm.201101-0004OC>
- Kumar, G., N. Kumar, A. Taneja, T. Kalekal, S. Tarima, E. McGinley, E. Jimenez, A. Mohan, R.A. Khan, J. Whittle, et al. Milwaukee Initiative in Critical Care Outcomes Research Group of Investigators. 2011. Nationwide trends of severe sepsis in the 21st century (2000–2007). *Chest*. 140:1223–1231. <http://dx.doi.org/10.1378/chest.11-0352>
- Li, P., M. Li, M.R. Lindberg, M.J. Kennett, N. Xiong, and Y. Wang. 2010. PAD4 is essential for antibacterial innate immunity mediated by neutrophil extracellular traps. *J. Exp. Med.* 207:1853–1862.
- Lowy, F.D. 1998. *Staphylococcus aureus* infections. *N. Engl. J. Med.* 339:520–532. <http://dx.doi.org/10.1056/NEJM199808203390806>
- Maguire, O., C. Collins, K. O’Loughlin, J. Miecznikowski, and H. Minderman. 2011. Quantifying nuclear p65 as a parameter for NF- κ B activation: Correlation between ImageStream cytometry, microscopy, and Western blot. *Cytometry A*. 79:461–469. <http://dx.doi.org/10.1002/cyto.a.21068>
- Matute-Bello, G., C.W. Frevert, O. Kajikawa, S.J. Skerrett, R.B. Goodman, D.R. Park, and T.R. Martin. 2001. Septic shock and acute lung injury in rabbits with peritonitis: failure of the neutrophil response to localized infection. *Am. J. Respir. Crit. Care Med.* 163:234–243. <http://dx.doi.org/10.1164/ajrccm.163.1.9909034>
- McDonald, B., R. Urrutia, B.G. Yipp, C.N. Jenne, and P. Kubers. 2012. Intravascular neutrophil extracellular traps capture bacteria from the bloodstream during sepsis. *Cell Host Microbe*. 12:324–333. <http://dx.doi.org/10.1016/j.chom.2012.06.011>
- Rohrbach, A.S., D.J. Slade, P.R. Thompson, and K.A. Mowen. 2012. Activation of PAD4 in NET formation. *Front. Immunol.* 3:360. <http://dx.doi.org/10.3389/fimmu.2012.00360>
- Scott, S.A., P.E. Selvy, J.R. Buck, H.P. Cho, T.L. Criswell, A.L. Thomas, M.D. Armstrong, C.L. Arteaga, C.W. Lindsley, and H.A. Brown. 2009. Design of isoform-selective phospholipase D inhibitors that modulate cancer cell invasiveness. *Nat. Chem. Biol.* 5:108–117. <http://dx.doi.org/10.1038/nchembio.140>
- Wang, Y., M. Li, S. Stadler, S. Correll, P. Li, D. Wang, R. Hayama, L. Leonelli, H. Han, S.A. Grigoryev, et al. 2009. Histone hyperacetylation mediates chromatin decondensation and neutrophil extracellular trap formation. *J. Cell Biol.* 184:205–213. <http://dx.doi.org/10.1083/jcb.200806072>
- Xiao, H., J. Siddiqui, and D.G. Remick. 2006. Mechanisms of mortality in early and late sepsis. *Infect. Immun.* 74:5227–5235. <http://dx.doi.org/10.1128/IAI.01220-05>